

Self-powered solar-driven zero liquid discharge desalination plant based on drum film evaporators

Vitaly Uzikov, <https://infoengineering.ru/>

Abstract

Millions of people suffer from a shortage of fresh water: the available resources rapidly reduce their capacity with the growing demand. Shortage of fresh water in several regions of the Earth is becoming a serious problem posing a threat to the mankind evolution and the environment conservation.

Water and energy scarcity are two major global challenges facing modern society. Right now, almost one-fifth of the world's population is living in areas with water scarcity, and another 1.6 billion people are living in economic water scarcity areas because of technical or financial limitations to getting freshwater even when water is available. So, water treatment techniques employing solar energy are deemed attractive for producing fresh water from impotable water sources, including seawater, river/lake water and contaminated water, by safe and sustainable methods.

Solar-driven desalination in the countries with hot and arid climate can employ abundant and free solar energy to produce freshwater from natural water sources, making this technology a promising one to solve the water scarcity problem.

Besides, solar-driven zero liquid discharge (ZLD) desalination from waste brine water has recently emerged as a new important application of solar evaporation. Compared with conventional ZLD desalination technologies, solar-driven ZLD desalination produces solid salt as the only byproduct and uses sunlight as the only energy source, making it less energy intensive, more cost-effective, and affordable.

This paper considers a concept of a small self-powered solar-driven multi-stage ZLD desalination plant based on film evaporation drums and having a desalination capacity of up to 1100 liters of freshwater per day.

KEY WORDS: solar energy, film evaporation drum, multi-stage evaporation, desalination, zero liquid discharge, energy conversion.

Introduction

Solar energy and water are the two most abundant resources on Earth. Nevertheless, water and energy scarcity are two major global challenges facing modern society. Right now, almost one-fifth of the world's population is living in areas with water scarcity, and another 1.6 billion people are living in economic water scarcity areas because of technical or financial limitations to getting freshwater even when water is available. This circumstance will be much more serious by the year 2025, when it is projected that two-thirds of the world's population will be under water stress conditions, according to the United Nations' World Water Development Report in 2012. Thus, a technology that combines the advantages of freshwater generation, easy accessibility, and cost-efficient energy input is of great interest for dealing with this global water crisis, especially for people living in off-grid areas [1].

Saline seawater is practically inexhaustible resource that makes up 97.5 % of the Earth's water, however, its use for household needs and as drinking water is problematic due to high concentration of salts dissolved in it.

It is no surprise then that one of the principal options to overcome freshwater scarcity is the construction of big industrial seawater desalination plants in the coastal areas, particularly, in the Middle East.

However, large-scale industrial desalination is not a cure-all solution to solve the water stress problem in certain regions of the world. According to the recent scientific research published by the UN, approximately 16 thousand desalination plants produce basically more toxic waste than freshwater. Saline suspension (or brine), that is a solution of extracted salts, contains a large amount of copper and chlorine. It is discharged back into the ocean or the sea as desalination is completed. The presence of chemicals employed in the desalination process makes this hypersaline substance even more toxic, as reported by the researchers in the *Science of the Total Environment*. As the result, dead zones appear in the discharge areas, representing vast oxygen-free water areas where neither marine plants nor animals breathing the oxygen dissolved in the water can survive. Besides, poisoned water raises the temperature of the coastal waters. And what is more, the discharged waste volume exceeds 1.5 times the volume of freshwater produced. Thus, the desalination waste in general reaches 50 billion cubic meters of toxic discharge worldwide every year. This amount of brine would be enough to cover the entire territory of Florida in 30 cm of discharge. According to the reported data, more than half of the brine waste is produced by the oil countries: Saudi Arabia (22%), the United Arab Emirates (20.2%), Kuwait (6%), Qatar (5.8%) [2].

It seems impossible, however, to completely abandon the use of desalination plants nowadays, because the population of many countries, including Africa, the Middle East, and island states, depends on desalination technologies. According to the UN data, an estimated quarter of population is living in areas with water scarcity. The situation is forecast to be much worse because of aquifers depletion.

Since 2015, the Global Risks Report of the World Economic Forum is noted to permanently recognize "water crises" as one of the global threats. The water stress has several causes, and the annually growing Earth's population is one of them. [2]

The currently in use industrial desalination technology has been existing since 1960s. A new ZLD desalination technology can possibly solve the problem of water resources contamination.

Conventional technologies are not capable of evaporating the feed till dry salt residue. Salt deposits on heating surfaces pose a major challenge connected with high salt concentration that hampers heat exchange and raises a need of frequent cleaning or mechanical descaling of the heating surfaces.

Salt deposits on the heating surfaces prevent from providing continuous and sustainable evaporation process leading to higher operational costs and poorer performance and efficiency of evaporation plants.

The proposed drum film evaporator-based (DFE-based) technology [4, 5, 6], providing the possibility of multi-stage evaporation and continuous mechanical descaling of the heating surfaces grants a solution to the major issues of solar-driven desalination, in particular:

- create ZLD desalination technology,
- achieve net-zero carbon emissions of desalination process,
- provide easy operation without sophisticated constructions and complex equipment,
- use a multi-stage desalination principle.

A zero liquid discharge problem can be solved in two stages. At the first stage, a DFE evaporates the feed to obtain high-concentration brine (approximately 300 g/L, which corresponds to a salt content of the Dead Sea water). This brine requires minimum cost to withdraw the entire unbound water and obtain dry solid salt, creating minimum problems with salt deposits on the evaporators' surfaces and in the drain piping. At the

second stage, the high-concentration brine is evaporated till solid dry salt on an open-air platform heated from below, where the moisture is removed from the brine into the atmosphere as due to the insolation on the platform, so as due to the heating of the platform with extraction steam supplied from the final DFE stage.

Thus, a new design of the solar-driven evaporator opens the possibilities for more environmentally friendly ZLD desalination, treatment of brines with high salt content at the conventional desalination plants, as well as purification of highly-saline industrial wastewater.

New type of evaporators

Many types of evaporators are known to be used in distillation, including:

- horizontal tube evaporators,
- horizontal spray film evaporators,
- long tube vertical evaporators,
- short tube vertical evaporators,
- basket type evaporators,
- forced circulation evaporators,
- agitated thin film evaporators or wiped film evaporator, and
- plate evaporators.

However, we propose a new type of evaporator to be employed in the problem of energy-effective solar-driven ZLD distillation of saline water, i.e. a drum film evaporator (DFE).

With respect to the abundant, renewable and widely spread solar energy and water sources, this environmentally-safe net-zero carbon process without sophisticated constructions makes solar-driven evaporation one of the most promising technologies to produce freshwater and to convert energy. The solar-driven multi-stage desalination plant under consideration is designed, first of all, for household (individual) application and, prospectively, for commercial application in the hot and freshwater deficient countries.

The feasibility of the technology under consideration was verified by computational analysis for favorable conditions of hot and arid climate, corresponding to the climate in Cairo, Egypt [3], (Figure 1).

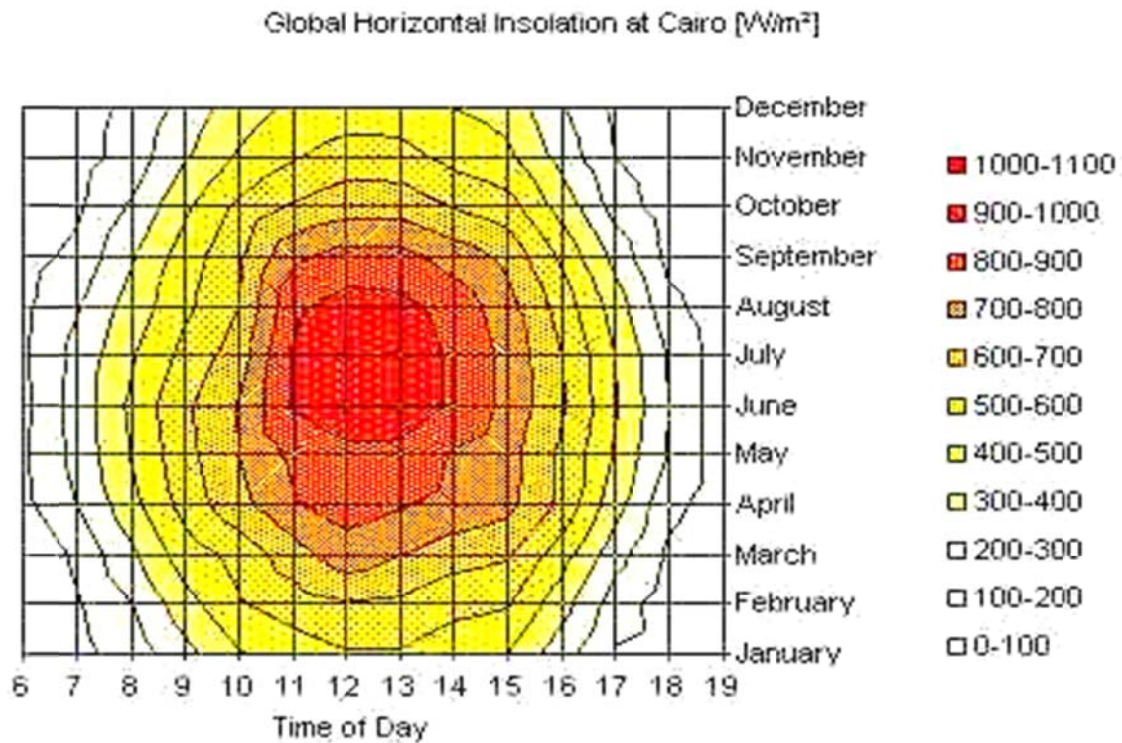


Figure 1 - Global insolation by months (December to January) and time of the day for Cairo, Egypt.

The diagram in the figure shows, that the maximum horizontal insolation in summer months can be up to 1.1 kW/m^2 in such a hot and arid region like Egypt, that is why the maximum predicted effectiveness is bound to the Middle East location.

A parabolic trough concentrator is chosen to use the solar energy with maximum efficiency and to reduce the complexity and cost of the design.



Figure 2 - A single-axis tracking parabolic trough collector.

The electrical energy supplied to the collector tilt drive, DFE rotation drives, solenoid valves, and the monitoring and control system can be taken as from the grid, so as from a stand-alone energy source, for example, from photovoltaic collectors (Figure 3).



Figure 3 - Flat-plate photovoltaic collector applications (Photo courtesy of DOE/NREL, Warren Gretz)

DFE-based evaporators have an advantage of modularity when individual standardized drum film evaporator modules (DFEM) [4, 5, 6] can be included into the process flow both in parallel and in series maintaining the predetermined performance. An option to choose a net-zero carbon energy source (for example, solar energy or evaporation following the mechanical vapor recompression technology) is also an important advantage.

DFEM features

The DFEM design is simple and manufacturable since large-diameter pipes, including conventional standard pipes with rather low cost are its basic components.

With modular evaporator plants being widely applied, the large-scale production of the modules will provide low production cost and thus low price of the standardized DFEMs which contribute the most to the general cost of the solar-driven multi-stage desalination plants.

A DFEM is a horizontal film evaporator-heat exchanger with a heated rotating drum. [4, 5, 6]. The drum is partially filled with the liquid to be evaporated which creates a film on the drum inner surface while the drum is rotating. The film is intensively evaporating while the heat is supplied to the external surface of the rotating drum and vapor is continuously removed from the drum. The similar process can be observed in laboratory-scale rotor evaporators during evaporation of solutions [11], when the vapor is removed from the flask by vacuuming and external heat is supplied to the outer surface of the flask from the hot liquid into which the flask is partially submerged and is rotating at an angle to the horizontal (Figure 4).



Figure 4 - Rotor evaporator LRE-20 (LABOAO)

Figure 5 helps to see the difference between a DFEM design and a rotor evaporator design. This difference lies in replacement of a flask rotating at an angle to the horizontal with a horizontal metal drum (1) on the ball bearings (2), thus enabling non-stop scraping the internal heating surfaces to remove the salt deposits under the liquid level (3), for example, by a rolling scraper featuring a rod with an auger-type winding (4). The sharp edges of the auger-type winding constantly contacting the internal drum surface impede the growth of salt deposits on the internal heat-exchanging surface. The auger rotation along with the drum rotation moves the generated solid debris to the point (5) where the salt concentrate is periodically discharged via a drain tube (6) upon reaching the predetermined concentration. This keeps the heating surface clean thus enabling continuous evaporation process. The loss of concentrate that occurs when periodically draining the concentrate via the drain tube is automatically compensated by the feed liquor. Concentrate bleeding and feed supply occur at the opposite ends of the drum, thus providing high salt concentration in the drained brine batches. The drum rotation speed is selected basing on the condition of the concentration increase in the film up to the optimal values and is maintained by an electric gear motor (7) being a part of the evaporation module equipment. Similar to the rotor evaporators, the drum is only partially filled with the process liquor (3) with its level maintained constant with a float valve (8) installed on the supply tube (9).

Figure 5 shows a cutaway view of the DFEM with a heating steam jacket and an auger-type scraper for cleaning the heating surface.

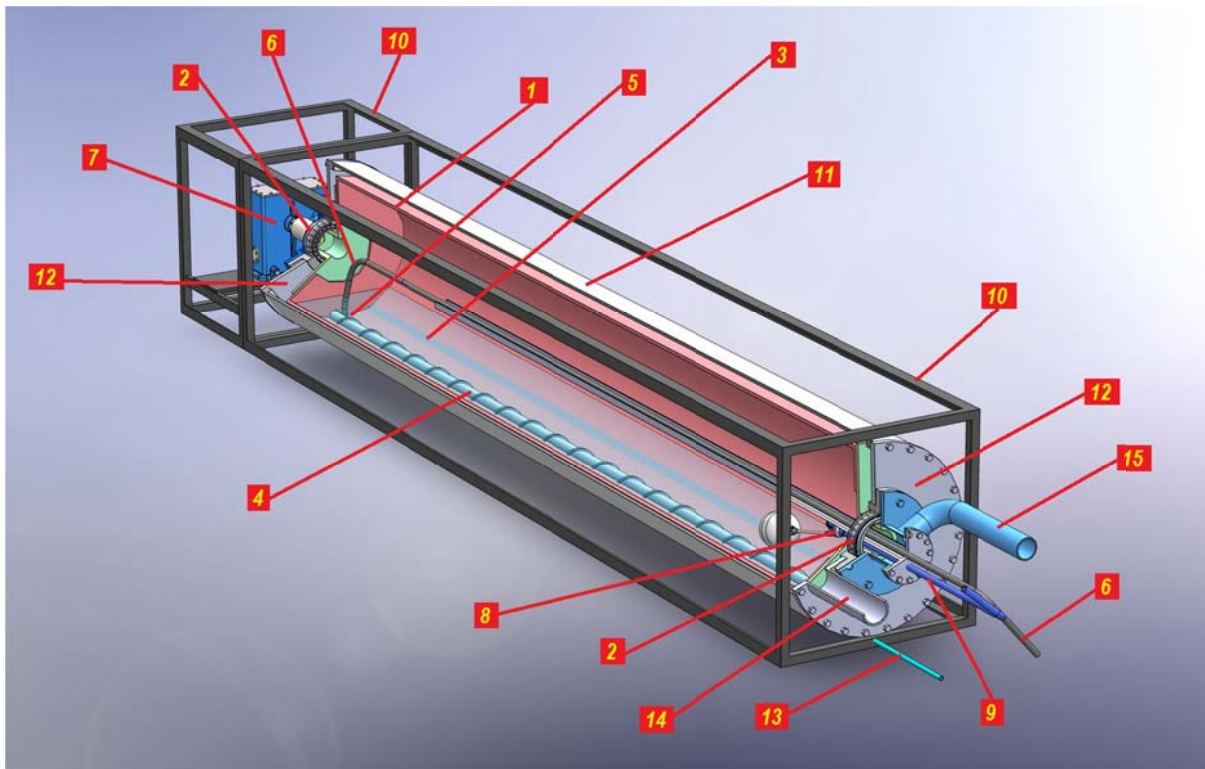


Figure 5 - Design of DFEM with a heating steam jacket and an auger-type scraper for cleaning the heating surface

The design of the DFEM with a heating steam jacket comprises a frame (10) housing an air-tight cylinder (11) with flanged ends (12) and a DFE rotation drive (7). Drain pipe (13) serves to drain the distillate occurring after the heating steam condenses on the external surface of the drum. The heating steam is supplied to the DFEM via a branch pipe (14), and the secondary steam is removed via a branch pipe (15).

Design of Self-Powered Solar-Driven Desalination Plant Based on Drum Film Evaporators

The solar-driven desalination plant follows the design of a multi-stage plant where the steam generated in the DFE at the first stage using the concentrated insolation energy becomes heating steam in the steam jacket of the standardized evaporation module of the first stage which is a part of a unit comprised of three series-connected DFEMs. The steam generated on the previous stage becomes the heating steam for the next one, that multiplies the process capacity with one and the same consumption of thermal energy. The steam generated at the final-stage DFEM during its condensation partly warms up the input water before it is fed into the evaporation drums and partly warms up the salt concentrate for open-air drying.

The process flow diagram of the solar-driven multi-stage desalination plant with the process streams is shown in Figure 6.

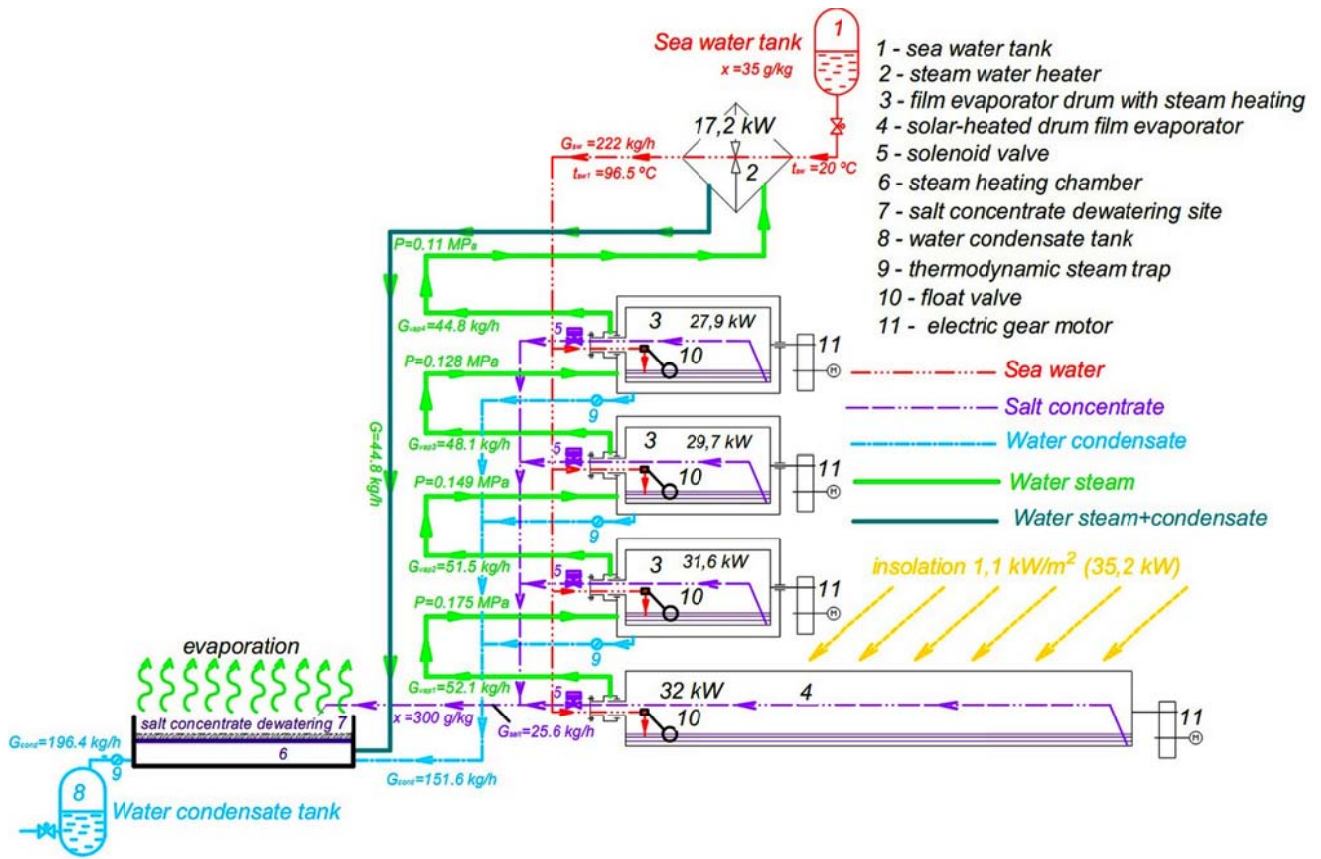


Figure 6 - SSDP-DFE process flow diagram

The desalination process is controlled by changing the position of the single-axis parabolic collector to track the sun as it moves across the sky, and by intermittently opening the solenoid valves to drain the concentrate on the open-air drying platform where dry salt is obtained. The concentrate is drained batchwise after its salt content reaches about 300 g/L. The volume of the drain batches depends on the unloading frequency and is adjusted in accordance with the on-site operation conditions.

No control is needed to drain condensate from the heating jackets of the modules and from the recuperative heat exchanger, since it is done via passive elements, i. e. thermodynamic steam traps [7]. The level of liquid in the drums is maintained automatically with float valves. Liquid streams are moved by hydrostatic pressure created because the feedwater tank is mounted at an elevation and the condensate receive tank is arranged at the lowest point of the desalination plant. These peculiarities enable easy control of the process without involving the operating personnel.

The only area of the desalination plant that appears to call for particular attention during its operation is the salt dewatering platform, since the dry product have to be regularly removed. The removal can be carried out as in manual way, so as mechanically by employing electrically-driven brushes moving across the salt dewatering platform.

Figure 7 shows a 3D model of SSDP-DFE with a capacity of up to 200 liters per hour.

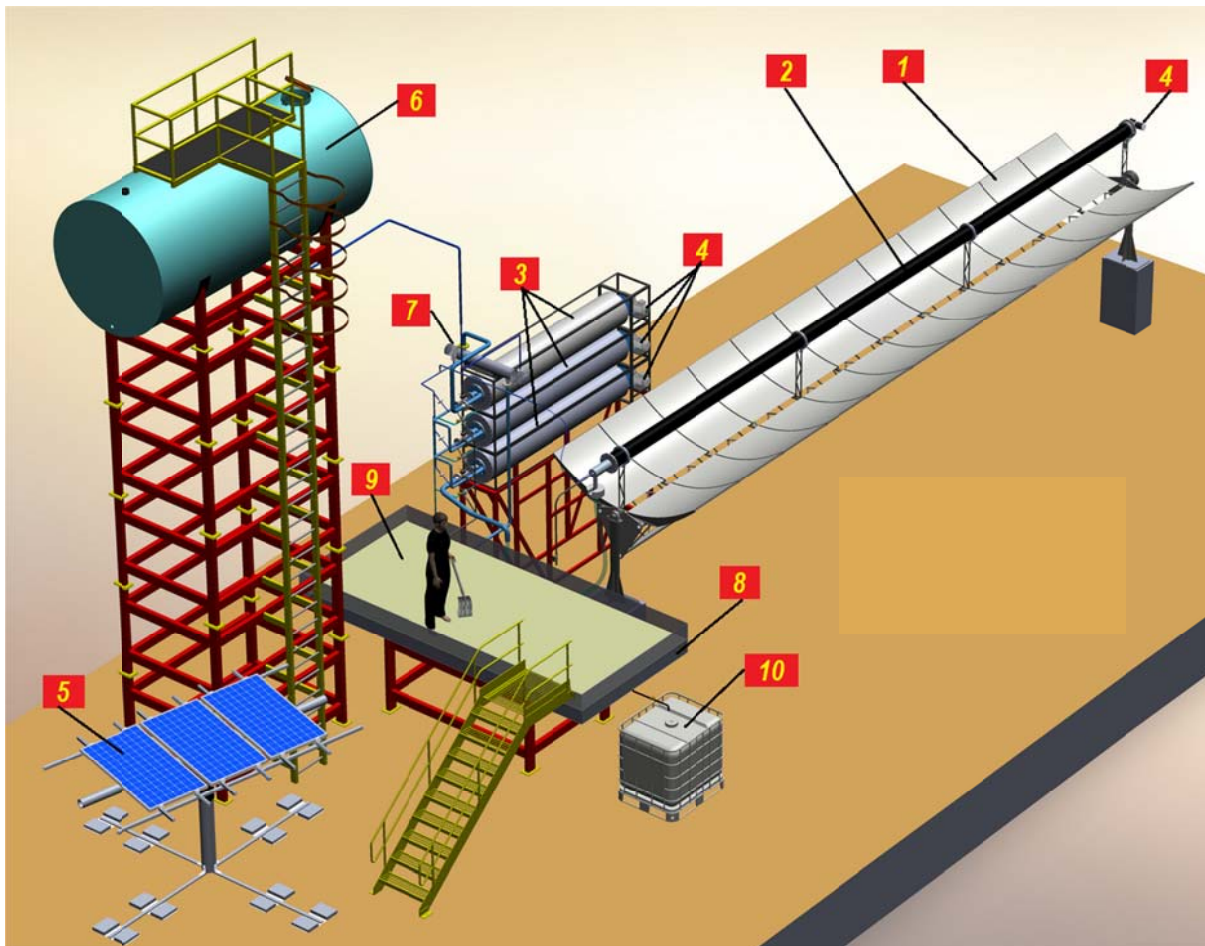


Figure 7 - 3D model of SSDP-DFE with a capacity of up to 200 liters per hour.

The first-stage drum is heated by the solar energy concentrated with the parabolic trough collector (1). The external surface of the drum has a light-absorbing layer (2) to enhance the absorption of thermal energy. It can be, for example black paint covering the aluminum surface of the drum, thus enabling the absorption of more than 90% of incident radiation [12]. Under the maximum solar irradiance $I = 1.02 \text{ kW/m}^2$, a parabolic collector with an area $A = 38 \text{ m}^2$ focuses $Q_{DFE} = 35.2 \text{ kW}$ of radiation energy on the drum, that corresponds to the thermal capacity for evaporation $Q_{ev} \sim 32 \text{ kW}$ (with respect to the emissivity coefficient ϵ' of the drum surface), giving the steam generating capacity $m = 52.05 \text{ kg/h}$ under the pressure $P = 0.175 \text{ MPa}$.

The drums of the next DFEM stages are heated with the steam generated on the previous stage. The steam condenses on the external surface of the drum, and the condensate leaves the heating jacket through a thermodynamic steam trap [7] by gravity and fills the space under the salt dewatering platform (9) (see Figure 7). The steam generated with the solar energy in the first-stage DFE is fed to the unit of three series-connected DFEMs (3) via a flexible hose. Since the plant is fully self-powered, all DFEMs are rotated by gear motors (4) powered by the flat-plate photovoltaic collector (5). Feedwater is supplied to the DFE from the feed tank (6) mounted at an elevation after pre-heating in the steam water heater (7). The heating steam for this steam water heater is taken from the final (the third) DFEM stage and partially condenses there. The rest of the steam is forwarded to the space (8) located under the salt dewatering platform (9) as a mixture of steam and water, where it is condensing while heating and drying the salt on the platform. This very space accumulates all hot condensate from all DFEMs which flows there via the piping with thermodynamic steam traps. Partially cooled, the total condensate stream from ASDP-DFE is drained from the space under the salt dewatering platform to the distillate tank (10).

The proposed design of the solar-driven evaporator considers four evaporation stages, where the first one uses solar energy to generate steam, while on the following three stages the secondary steam is generated using the steam from the previous stage with higher pressure, and, consequently, higher temperature, than the current stage steam.

Figure 8 shows the design of a DFE-based evaporation module heated with a parabolic trough collector. The external surface of the DFE is covered with a layer of light-absorbing paint (1) [12]. The parabolic trough collector and the first-stage DFE are mounted on the bearing supports (2) to enable their rotation. The feedwater is supplied via a flexible tube (3) and the salt concentrate is removed via tube (4) with a solenoid valve (12). The steam generated in the DFE is removed to the three-DFEM unit via a branch pipe (5) and flexible tubing (6). A load (7) is used to keep the branch pipe (5) upright while the parabolic trough collector is rotating. The feedwater is supplied through a float valve (8) keeping a constant water level (9) in the DFE. A gear motor (10) rotates this DFE, an auger-shaped rod (11) tumbles under the water level, thus removing the salt deposits inside the drum. When the brine batch reaches the required salt concentration, the batch is drained to the salt dewatering platform by intermittently opening the solenoid valve (12).

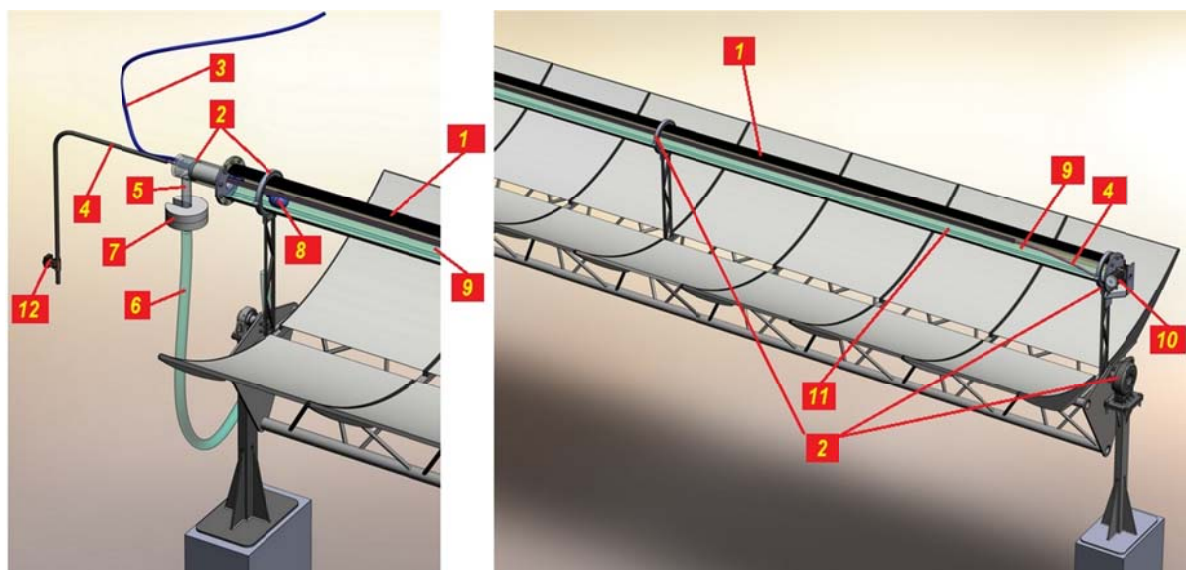


Figure 8 - DFE-based evaporation module heated with a parabolic trough collector.

The piping of the solar-driven desalination plant is shown in Figure 9.

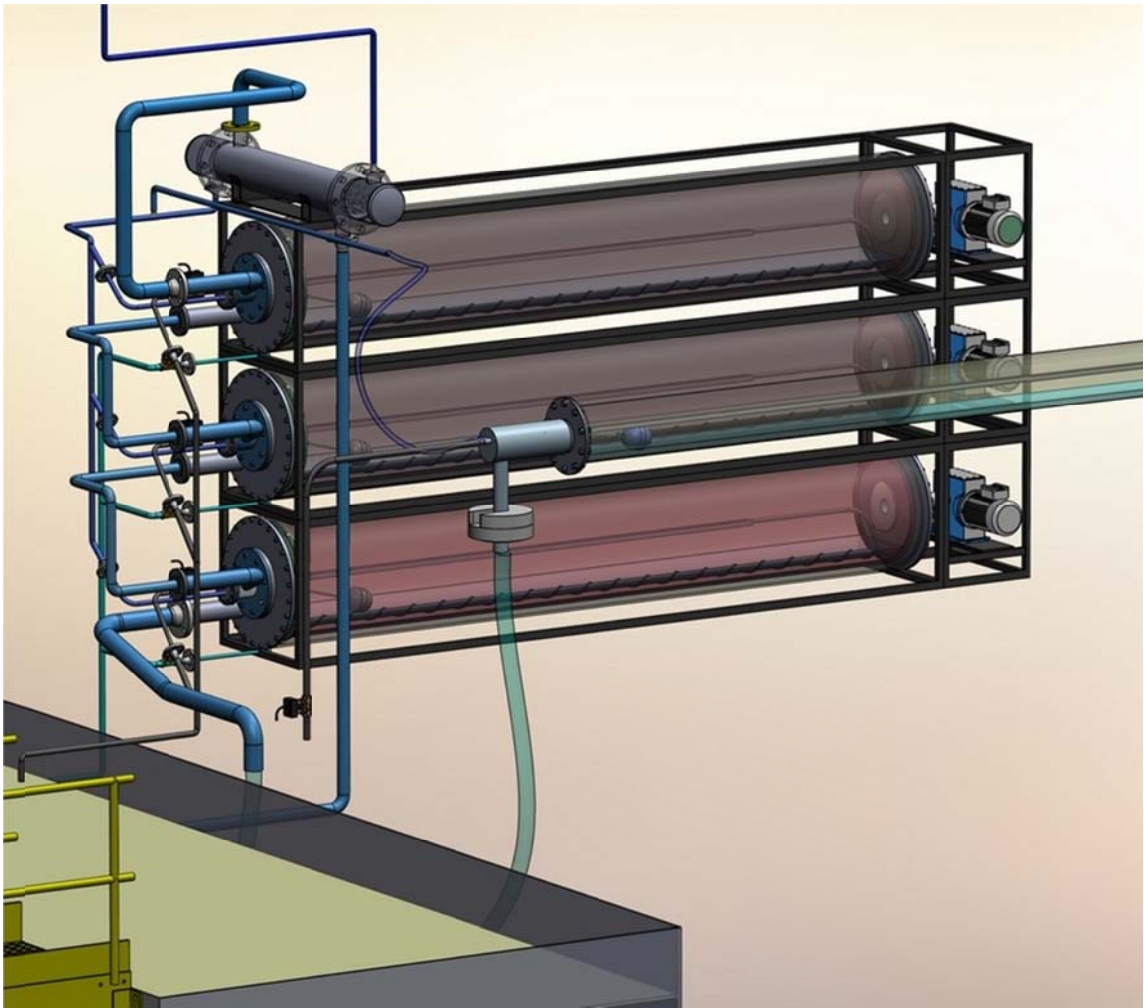


Figure 9 - The piping of the solar-driven desalination plant

Connection of the steam water heater to the pipelines is shown in Figure 10.

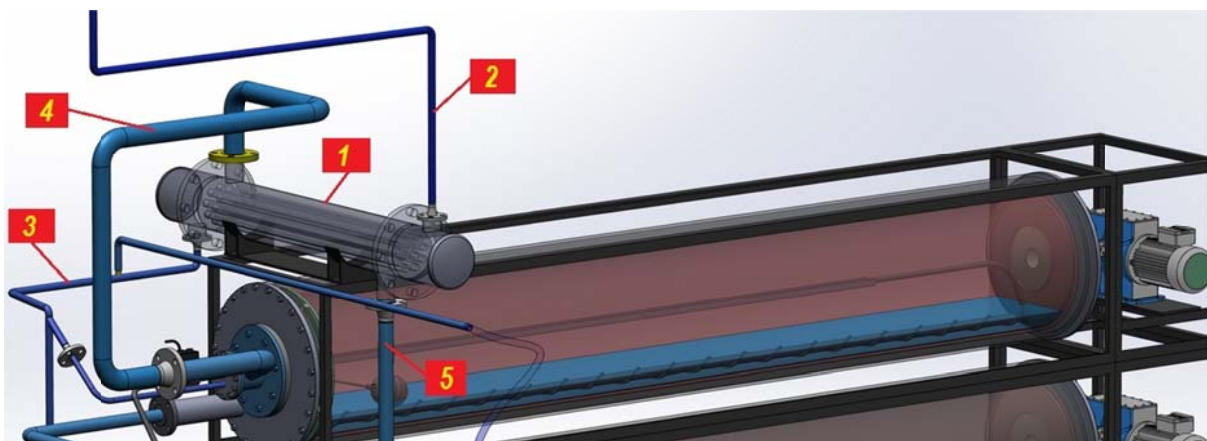


Figure 10 - Connection of the steam water heater to the pipelines

The feedwater is supplied to the steam water heater from the tank through a tube (2). It passes the tube side of the horizontal shell-and-tube heat exchanger and then, heated up, is distributed to all DFEs through the tube (3). The feedwater is heated with the secondary steam supplied from the final DFEM stage by the steam

line (4) to the shell side of the steam water heater. After it partially condenses, a mixture of water and steam runs to the space under the salt dewatering platform (2 in Figure 11) via the pipeline (5).

Figure 11 shows the design of the salt concentrate dewatering area, comprising an open-air dewatering platform (1) where salt concentrate is intermittently drained from tubes (3) and (4) after opening solenoid valves (8). There is a heating space (2) under the dewatering platform, where the rest of the steam leaving the steam water heater by pipe (6) condenses. This space also receives hot condensate via pipe (5).

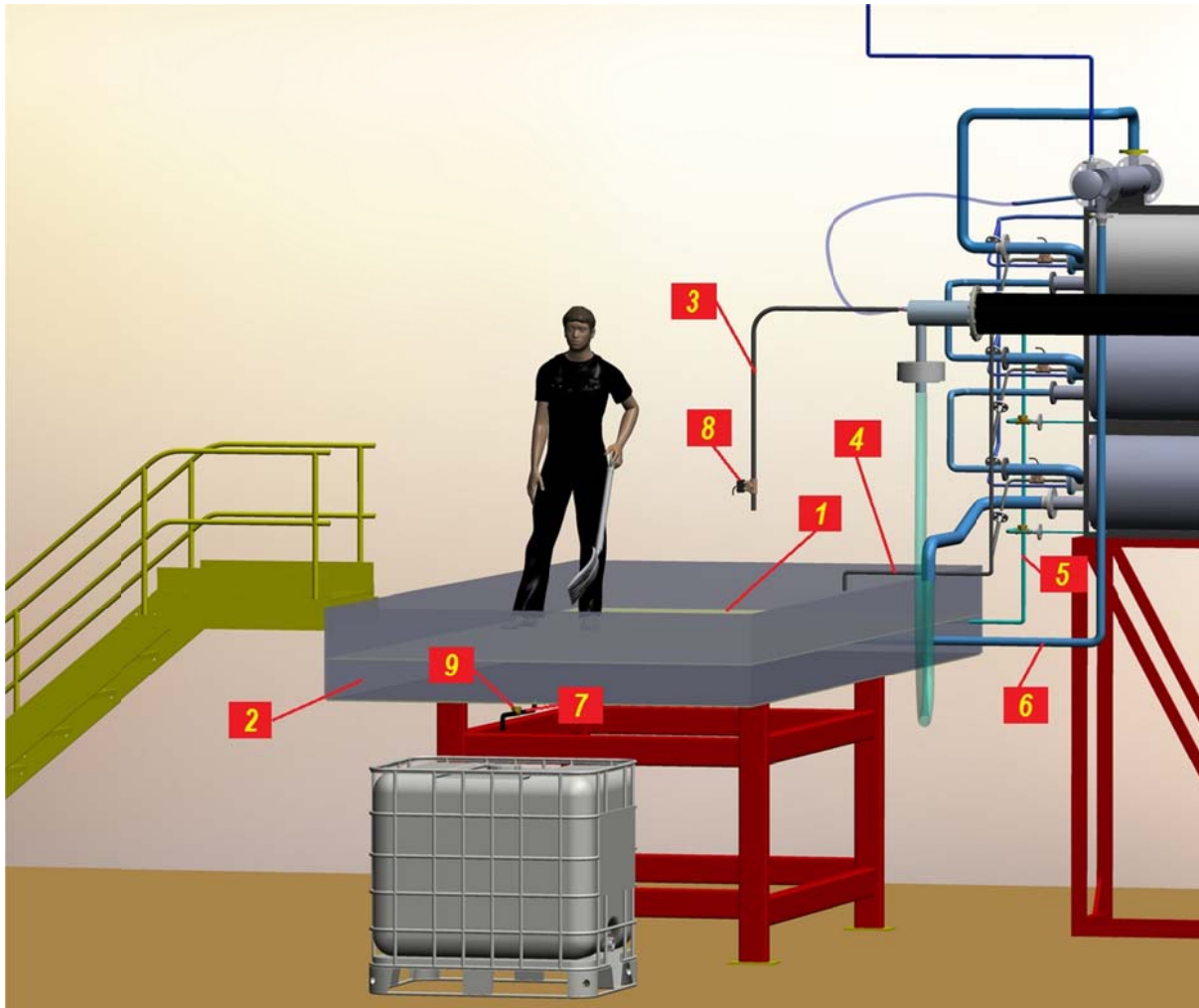


Figure 11 - The design of the salt concentrate drying area

The total condensate stream from the heating space under the salt dewatering platform (2) is drained to the distillate tank via the tube (7) with a thermodynamic steam trap (9).

Results and discussion

Analysis of the parameters of the solar-driven desalination plant with the maximum capacity up to 200 liters per hour

The estimation of the SSDP-DFE capacity requires determining the thermal transfer rate in the DFE and the material balance of the desalination process.

The heat transfer coefficient α [$W/(m^2 \cdot K)$] for steam condensation on the external surface of the rotating drum is calculated by formula [4] derived for laminar film motion (conservatively):

$$\alpha_{conc} = 0,728 \times \sqrt[4]{\frac{g r \rho \lambda^3}{\nu_w d_2 \Delta t_{wv}}} \quad (1)$$

where

where g is the free fall acceleration, m/s^2 ;

r is the specific heat of steam generation, kJ/kg ;

ρ is the water density kg/m^3 ;

λ is the thermal conductivity, $W/(m \cdot K)$;

ν is the kinematic viscosity of water, m^2/s ;

Δt_{wv} is the temperature difference on the fluid film, $^{\circ}C$;

d_2 is the outer diameter of the evaporation drum, m .

According to [14], the heat transfer coefficient of the film evaporators with the surface evaporation for $q < 8 kW/m^2$, $Re = 2000 \dots 8000$ and $\Gamma = 400 \dots 2000 kg/(m \cdot h)$ is recommended to be selected using the equation

$$\alpha_{ev} = 0,0067 \frac{\lambda_w}{\delta_w} (0.25 Re)^{0.56} \quad (2)$$

Where

λ_w is the thermal conductivity of fluid film, $W/(m \cdot K)$;

δ_w is the thickness of the liquid film, m ;

Re is Reynolds criterion for fluid film.

The fluid film thickness is determined by the ratio [14]

$$\left(\frac{3}{4} \frac{v^2}{g}\right)^{1/2} Re^{1/3} \quad (3)$$

where v is the kinetic viscosity of the solution, and g is the gravitation constant.

Reynolds criterion for fluid film is determined by the ratio [14];

$$Re = \frac{4\Gamma}{\mu} \quad (4)$$

Where μ is the dynamic viscosity of the solution, and Γ is the linear mass irrigation density, defined by the formula [14]

$$\Gamma = \frac{G}{\Pi} \quad (5)$$

Where G is the solution flowrate and Π is wet perimeter

Since the drum is incompletely filled, the film evaporation area is taken 15% reduced, so the heat transfer coefficient of the evaporation used in the calculations is corrected accordingly.

The heat transfer coefficient of the drum walls is determined by the formula

$$K = \frac{0,85}{\frac{1}{\alpha_{conc}} + \frac{\delta_{wall}}{\lambda_{wall}} + \frac{\delta_{dep}}{\lambda_{dep}} + \frac{1}{\alpha_{ev}}} \quad (6)$$

Let us estimate the material balance of the desalination process. The material balance equation of the evaporation process is [9]:

$$G_{sw} = G_{conc} + W \quad (7)$$

$$G_{sw}x_{sw} = G_{conc}x_{conc} \quad (8)$$

Here G_{sw} , G_{conc} are the mass flowrates of the input (seawater) and the output (evaporated concentrate), kg/s ;

x_{sw} , x_{conc} are the mass fractions of the dissolved solids in the input and in the output;

W - is the mass flowrate of evaporated water, kg/s .

Setting the final concentration, one can calculate the mass flowrate of distillate:

$$W = G_{sw} \left(1 - \frac{x_{sw}}{x_{conc}} \right) \quad (9)$$

The heat-balance equation of the evaporator is [9]:

$$Q + G_{sw}c_{p\ sw}t_{sw} = G_{conc}c_{p\ conc}t_{conc} + Wi_{sec} + Q_{wast} \mp Q_d \quad (10)$$

Where Q is the thermal power for evaporation, W ;

$c_{p\ sw}$, $c_{p\ conc}$ is the specific thermal capacity of the input (seawater) and the output (evaporated concentrate), $J/(kg\ K)$;

t_{sw} , t_{conc} is the temperature of the input (seawater) at the DFE input and the output (evaporated concentrate) at the DFE output, $^{\circ}C$;

t_{sec} is the specific enthalpy of the secondary steam at the evaporator output, J/kg ;

Q_{wast} is the thermal power to compensate the wastage to the environment, W ;

Q_d is the dehydration heat, W .

Thus, the thermal power for evaporation is [9]

$$Q = G_{sw}c_w(t_{conc} - t_{sw}) + W(i_{sec} - c_{p\ w}t_{conc}) + Q_{wast} \quad (11)$$

Where c_w is the specific thermal capacity of water at t_{conc} , $J/(kg\ K)$.

The specific thermal capacity of water in two-component aqueous dilute solutions (water + diluted solid) ($x < 0.2$) is calculated using the approximation $c_p = 4190(1 - x)$, where 4190 [J/(kg K)] is the specific thermal capacity of water; x is the concentration of the diluted solid, [mass fractions].

For seawater, the fraction of NaCl (sodium chloride) is approximately 86%, so the value for sodium chloride $c_{p, NaCl} = 854$ J/(kg K) is assumed as the thermal capacity of anhydrous solution [10].

As for two-component concentrated aqueous solutions, the calculations use the formula [9]:

$$c_p = 4190(1 - x) + c_{p, NaCl}x, \quad (12)$$

where $c_{p, NaCl}$ is the specific thermal capacity of the anhydrous diluted solid (assumed for NaCl), J/(kg K).

The maximum evaluation of the SSDP-DFE performance was carried out for a hot region. As an example, Figure 12 shows the insolation over a full clear March day at Daggett, California, a meteorological measurement site close to the Kramer Junction solar power plant [3]. The outer curve representing the greatest rate of incident energy, shows the energy coming directly from the sun (beam normal insolation) and falling on a square meter of surface area. The peak rate of incident solar energy occurs around 12:00 noon and is 1,030 Watts per square meter. Over the full day, 10.6 kilowatt-hours of energy have fallen on every square meter of surface area as represented by the area under this curve [3].

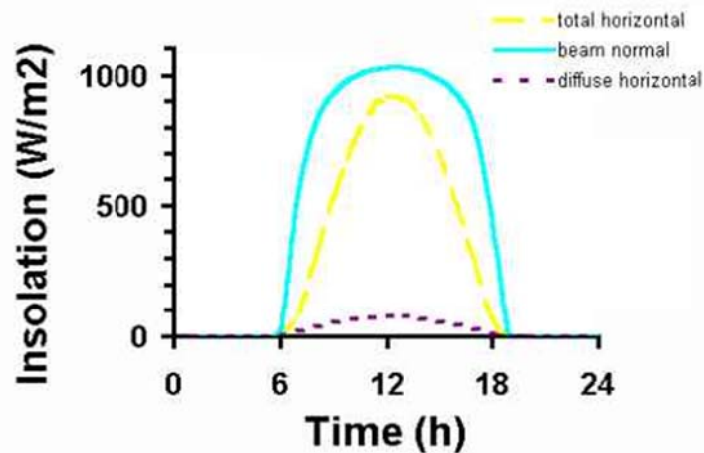


Figure 12 - Insolation data from Daggett, California on a clear March day [3].

The specifications of the solar-driven desalination plant are considered for a 200 liter-per-hour capacity plant with a 12-meter long parabolic collector mirror having an area 38 m² (Figure 7). The length of the rotating DFE on which the parabolic collector focuses the solar energy is also 12 m, and is 220 mm in diameter.

The principal specifications of the DFEMs assumed in the analysis are as follows:

| | |
|--------------------------------------|-----------|
| Housing material | aluminum; |
| Inner diameter, m | 0.42 |
| Wall thickness, m | 0.01 |
| Outer diameter, m | 0.44 |
| Heating surface length, m | 3.5 |
| Evaporation surface, m ² | 4.5 |
| Condensation surface, m ² | 4.84 |

Secondary steam parameters in the DFEM are determined by the pressure of the primary steam, thermal resistance, and heat-exchanging area of the drums. The DFE structure used in the analysis features a 3.5 mm long aluminum pipe with external diameter of 440 mm and a wall thickness of 10 mm. The area of the DFE heat-release surface makes up:

$$A_{DFE} \approx 3.14 \times 0.43 \times 3.5 \approx 4.7 \text{ m}^2$$

The thermal resistance of the drums is determined by the heat transfer coefficients for heating steam condensation on the external DFE surface and for evaporation of the solution from the film on the internal surface, as well as by the thermal resistance of the thin salt deposit layer with the thermal conductivity assumed as $\lambda_{\text{dep}} = 1.1 \text{ W/(m K)}$ (the deposit thickness was assumed 0.15 mm in the calculations) and the thermal resistance of the aluminum wall with the thermal conductivity $\lambda_{\text{wall}} = 150 \text{ W/(m K)}$ with the wall thickness $\delta_{\text{wall}} = 0.01 \text{ m}$.

To obtain the maximum thermal capacity, the steam generated in the "solar" DFE successively passes through three DFEMs, and the total pressure difference of the heating and secondary steam in these modules should not exceed the maximum pressure of the heating steam in the "solar" DFE. This pressure is determined either by the hydrostatic pressure of the water input to the "solar" DFE from the elevated water supply tank (as considered in this case), or by the input water pressure in the input water distribution system.

For the case under consideration where the water supply tank is located at an elevation of 8 m, Table 1 gives the calculated distribution of parameters in three DFEM stages, the first of which is heated by the steam under the pressure of 0.175 MPa with the flow rate of 52.1 kg/h.

Table 1 - Calculated distribution of parameters in three DFEM stages

| Parameters | Value | | |
|--|-------------|--------------|-------------|
| | first stage | second stage | third stage |
| Heating steam pressure, P_1 , [MPa] | 0.175 | 0.149 | 0.128 |
| Secondary steam pressure, P_2 , [MPa] | 0.149 | 0.128 | 0.110 |
| Steam pressure difference, ΔP , [MPa] | 0.026 | 0.022 | 0.018 |
| Saturation temperature, t_{sat} , [K] [°C] | 389.0 | 384.2 | 379.6 |
| | 116.0 | 111.2 | 106.6 |
| Temperature difference, Δt , [°C] | 4.81 | 4.63 | 4.44 |
| Heat transfer coefficient for steam condensation, α_{conc} , [W/m ² K] | 5282.3 | 5245.1 | 5203.9 |
| Calculated heat transfer coefficient for evaporation, α_{ev0} , [W/m ² K] | 4993.9 | 4741.9 | 4498.9 |
| Assumed heat transfer coefficient for evaporation, α_{ev0} , [W/m ² K] | 4244.8 | 4030.6 | 3824.0 |
| Thermal resistance for condensation $1/\alpha_{\text{conc}}$, [(m ² K)/W] | 0.000223 | 0.000224 | 0.000226 |
| Thermal resistance for evaporation $1/\alpha_{\text{ev}}$, [(m ² K)/W] | 0.000277 | 0.000292 | 0.000308 |
| Thermal resistance of DFE wall, $\delta_{\text{wall}}/\lambda_{\text{wall}}$, [(m ² K)/W] | 0.000067 | 0.000067 | 0.000067 |
| Thermal resistance of salt deposits, $\delta_{\text{dep}}/\lambda_{\text{dep}}$, [(m ² K)/W] | 0.000136 | 0.000136 | 0.000136 |
| Heat transfer coefficient, K , [W/m ² K] | 1422.67 | 1390.41 | 1357.30 |
| Heat flux density, q_{wall} , [kW/m ²] | 6.85 | 6.44 | 6.03 |

| | | | |
|--|--------|--------|--------|
| Transmission, [W] | 31632 | 29744 | 27860 |
| Mass flow rate of evaporated water, [kg/s] | 0.0143 | 0.0134 | 0.0124 |
| [kg/h] | 51.45 | 48.09 | 44.78 |

Taking into account the steam (condensate) produced in the "solar" DFE at 32 kW (steam generation heat at 0.175 MPa is 2213 kJ/kg), the total mass flow rate of the condensate produced by the plant is

$$W = \frac{32 \text{ kW} \times 3600 \text{ s}}{2213 \text{ kJ/kg}} + 51.45 \text{ kg/h} + 48.09 \text{ kg/h} + 44.78 \text{ kg/h} = 196,4 \text{ kg/h}$$

The required flow rate of seawater to concentrate the seawater with the initial salt concentration of 35 g/kg up to the Dead Sea concentration (300 g/kg) can be found by the formula (9)

$$G_{sw} = \frac{W}{\left(1 - \frac{x_{sw}}{x_{conc}}\right)} = \frac{196,4}{1 - \frac{35}{300}} = 222,3 \text{ kg/h}$$

In this case the flow rate of concentrate makes up

$$G_{conc} = 222,3 \frac{\text{kg}}{\text{h}} - 196,4 \frac{\text{kg}}{\text{h}} = 25,9 \frac{\text{kg}}{\text{h}} = 0,0072 \frac{\text{kg}}{\text{s}}$$

If the vaporation thermal capacity drops lower than 32 kW in the "solar" DFE, the vaporation intensity of the entire plant will decrease along with the total pressure difference (and, therefore, temperature differences) across all DFEMs.

Using steam water heater to increase the capacity of the solar-driven evaporation plant

Pre-heating of the input water before it enters the DFE increases the plant capacity. This is achieved by employing a steam water heater which uses the secondary steam of the final DFEM stage as heating steam. In the case under consideration, the steam heater features a horizontal shell-and-tube heat exchanger with 64 tubes $\varnothing 14 \times 1$ mm and 1.5 m long. Steam is supplied to the shell side, partially condenses thus heating the water from the feedwater tank which runs in the tubes up to 96.5°C, this water is then distributed to the DFEMs for evaporation. Large heat-exchanging area makes such heat exchanger immune to salt deposits on the internal surfaces of the heat-exchanging tubes, and the design allows easily removing the salt deposits from the tubes, if required.

Predicted parameters of the steam water heater (Figure 10) are shown in the heat transfer fluid diagram in Figure 12.

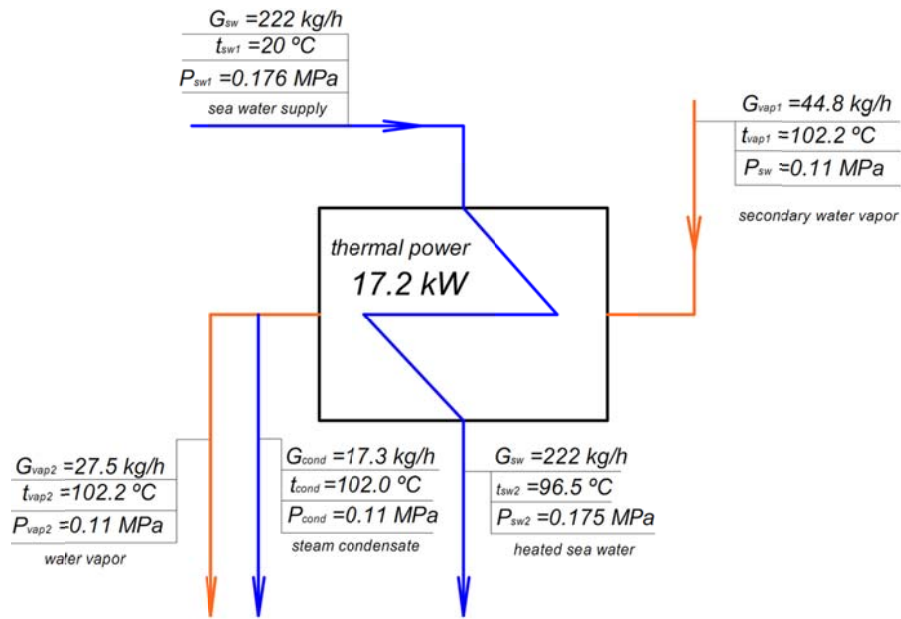


Figure 13 - Heat transfer fluid diagram of a steam water heater

After feedwater pre-heating and partial condensation of steam, the steam-condensate mixture from the shell side is supplied to the space under the salt dewatering platform where the remaining steam, while condensing, is heating the salt concentrate on the platform.

Beside the heat supplied to the dewatering platform by a stream of steam-water mixture from the steam water heater (~11 kW), the platform is also heated due to solar insolation. If the platform area is 10 m² (2 m × 5 m), the solar energy flux falling on the platform can reach 11 kW. Part of the solar heat is reflected, but even if the salt concentrate absorbs only 60% of the solar energy, ~ 6.6 kW of thermal energy is added to the steam heating to dry the salt concentrate.

Subject to the fact that the remaining steam from the heat exchanger condenses under the platform (flow rate 17.3 kg, steam generation heat 2250 kJ/kg), additional heating of the dewatering platform is provided with the thermal capacity

$$Q_{cond2} = \frac{17.3 \text{ kg/h}}{3600 \text{ s}} \times 2250 \frac{\text{kJ}}{\text{kg}} = 10,8 \text{ kW}$$

The total heat supplied to the platform to dry the concentrate (taking into account partial cooling of condensate) makes up at least

$$Q_{sum} = 6,6 \text{ kW} + 10,8 \text{ kW} = 17,4 \text{ kW}$$

To dehydrate the salt concentrate with the initial concentration of $s = 0.3 \text{ kg/kg}$, the flow rate of unbound water to be removed as steam can be found by the formula (9)

$$G_{out} = G_{conc} \left(1 - \frac{0.3}{1}\right) = 0,0072 \frac{\text{kg}}{\text{s}} \left(1 - \frac{0.3}{1}\right) = 0,00636 \frac{\text{kg}}{\text{s}}$$

To evaporate the water with this flow rate given the steam generation heat of 2258 kJ/kg the following thermal capacity is required

$$Q_{ev} = 0,00636 \frac{\text{kg}}{\text{s}} \times 2258 \frac{\text{kJ}}{\text{kg}} = 14,37 \text{ kW}$$

Thus, the total heat accepted by the platform from insolation and from the condensation of the third-stage steam is excessive, so the concentrate has to be moved from the DFE before the salt content reaches 0.3 kg/kg, particularly at $s = 0.247$ kg/kg. In this case, the throughput of seawater with the concentration of $s = 0.035$ kg/kg will increase from 222.3 to 228.7 kg with the output of condensate unchanged. This decrease in salt content of drained concentrate provides more favorable conditions to impede salt depositing on the heat-exchanging surfaces.

Since the insolation conditions and, thus, the thermal conditions of the dewatering platform, can vary during the day, the need for draining a concentrate batch can be easily determined by measuring the humidity of the air above the platform.

If the salt on the platform has already dried (the humidity detectors register low air humidity directly above the platform), short-time opening of the solenoid valve is needed to drain a batch of concentrate from the DFE onto the platform.

Cost-benefit evaluation of the proposed solar-driven evaporation technology

Practically negligible operating costs can be considered as an advantage of the proposed technology, since it contains absolutely no consumables such as sorbing agents, membranes, filtering materials, chemicals, including toxic ones, etc.). The only regular operation which requires human involvement is the removal of dry or semi-dry salt from the dewatering platform, and which, however, can be easily automated.

The components design is rather easy to manufacture and transport, the plant modularity significantly reduces the cost of individual DFEMs in scaled-up production.

The cost-benefit evaluation of the plant can be carried out by rough cost calculation of the plant with predicted performance. The cost estimate of the basic structural components of the plant is given below.

| Materials & Equipment | \$ |
|---|-----------------|
| A single-axis tracking parabolic trough collector | 8000 |
| Gear motors | 500 |
| Drums and hulls | 4700 |
| Flange designs | 5000 |
| Bearings | 1500 |
| Valves | 1800 |
| Frame | 1000 |
| The solar panel | 1000 |
| Tanks | 600 |
| Concentrate dewatering platform | 1100 |
| Pipelines | 400 |
| Mounting | 1500 |
| Total Installation Cost | \$ 27100 |

Since the plant is designed (due to its low efficiency) primarily for household (individual) application, we do not consider the maintenance-related costs in the estimation.

The average daily desalination output would be approximately 1.2 m^3 of freshwater, the annual output - 429 m^3 for hot regions with the average annual insolation of 2300 (kWh)/m^2 . During the expected service life of 60 years, the plant can produce 25730 m^3 of freshwater. Then, with the predicted plant cost of \$27.1 thousand, the specific water production cost will be approximately \$1.05 per cubic meter. Easy operation and no need of consumables can make this cost acceptable.

Besides, one more substantial argument for using such plants exists. This solar-driven evaporator is not only self-sufficient in terms of energy (not bound to any centralized power-supply source), has net-zero carbon emission, and operates using zero liquid discharge technology, it is "omnivorous" as well and is apt to desalinate and recover brines from the industrial plants that use brackish water reverse osmosis (BWRO) desalination and sea water reverse osmosis (SWRO) desalination. With this ability, the plant can solve a daunting environmental issue of dead zone formation in brine discharge areas.

Conclusion

Recently, there has been an ever-growing interest in ZLD desalination technologies, since they are expected to be an environmentally acceptable means to recover concentrated brine obtained in SWRO, in particular, in inland regions where other more conventional recovery options are inexpedient [15]. Usually, the techniques to convert liquid concentrate into solid include evaporation pools, crystallizer pans, and spray driers. The concentrate shall be treated to prevent scale build-up during secondary reduction, then the brine is concentrated and dried [16].

The final concentration of brine and evaporation steps employed in the currently-used technologies are very expensive, as a rule, since they are very energy-intensive, have significant carbon footprint or, in case of evaporation ponds, require large acreage. So, as a rule, commercial recovery of salts in the existing ZLD systems does not make economic sense. Dust salt carried out by the wind and provoking the neighboring soil salinization is an environmental issue for evaporation ponds.

A frenetic change of the desalination technology in the SSDP-DFE plant powered exclusively by solar energy will give a solution to the problem of environmentally-friendly ZLD desalination. A shift to relatively inexpensive low-efficient but easily maintained plants with expected dry salt output can relieve a majority of current problems attributed to desalination plants.

First of all, the SSDP-DFE technology is aimed mainly at household (individual) application in semi-arid and extremely arid regions of the planet, since it allows using brines from Sea Water Reverse Osmosis (SWRO) desalination as feedwater, thus solving the discharge problem. Transportation expenses to deliver brine to SSDP-DFE plants can be an affordable price for the solution of the acute environmental problem.

An SSDP-DFE belongs to small desalination plants with the capacity of $< 10 \text{ m}^3$ per day, however, the energy intensity of this thermal desalination technology makes the plant viable enough.

Notwithstanding multiple thermal desalination processes used, multi-stage flash (MSF) desalination is the most widely employed one, while MED and mechanical vapor compression desalination find limited use. Moreover, even MSF is not exhibiting significant expansion nowadays, and is just upholding its status quo at desalination market. This is connected with a relatively higher SEC of these processes as compared to RO. According to the study, MSF SEC and MED SEC were estimated as 18 kWh/m^3 and 15 kWh/m^3 , respectively, while RO SEC was 5 kWh/m^3 [17].

Since the gear motors for DPE rotation have high gear ratio, and the rotation speed of the drums does not exceed 10 revolutions per minute, the energy consumption is not more than 0.5 kW, thus the daily energy consumption to produce one cubic meter of freshwater will not exceed 5 kWh (SEC of ASDP-DFE was ~ 5

kWh/m³). This is a very favorable specific energy consumption value even setting aside the fact that this energy can be obtained from photovoltaics almost for free.

The application of fool-proof modular SSDP-DFEs that do not require any consumables for desalination process will promote their wider use in the households even notwithstanding their low efficiency, and that, in its turn, will pave the way for scaled-up production of such desalination plants and cost reduction.

References

1. Chaoji Chen, Yudi Kuang, Liangbing Hu, **Challenges and Opportunities for Solar Evaporation**, Joule, Volume 3, Issue 3, 20 March 2019, Pages 683-718
2. Contemporary desalination plants pollute the ocean with toxic waste, scientists say./ <https://voda.org.ru/news/science/sovremennye-opresnitelnye-ustanovki-zagryaznyayut-okEAN-toksichnymi-otkhodami-schitayut-uchenye/>
3. William B. Stine, Michael Geyer, Power From The Sun. Part 2. Solar Collectors / <https://www.rlocman.ru/review/article.html?di=68277>
4. Film evaporation drum, Patent RU 2761207 C1, 2021.
5. Emission installation for concentration of liquid solutions. Patent RU 2619768 C1, 2021.
6. Concentration of liquid solutions, Patent RU RU 2488421 C1, 2012.
7. Bhatia A., Overview of Steam Straps, / <https://www.cedengineering.com/userfiles/Overview%20of%20Steam%20Traps-R1.pdf>
8. Shiryaev Yu. N., Mitropov V.V. Analyzing a horizontal shell-and-tube condenser of a refrigerating unit: Study Guide. -Spb.: ITMO University, 2016. - 58 pages.
9. Pavlov K. F., Romankov P. G., Noskov A. A. / Case studies and problems of the Chemical Technology Processes and Equipment Course. Textbook for higher education / Edited by Romankov P. G., associate member of the USSR Academy of Sciences. — 10th Edition — L.: Khimiya, 1987. - 576 p, ill.
10. NaCl (sodium chloride) material / http://electrosteklo.ru/NaCl_rus.htm
11. J. T. Sharp, I. Gosney, A.G. Rowley, Practical Organic Chemistry / Translated into Russian by V. A. Pavlov, edited by V.V. Moskva. — M.: Mir, 1993. — ISBN 5-03-002126-4.
12. Emissivity factor and light-absorbing ability of materials / <https://msd.com.ua/energija/sepen-chernoty-i-pogloshhatelnaya-sposobnost-materialov/>
13. Principal processes and equipment of chemical technology. Engineering design handbook / Edited by Yu. I. Dytynsky. — M.: Khimiya, 1983. 272 p, ill.
14. Tananayko Yu. M., Vorontsov Ye. G., Analysis and research methods of film processes. Kyev.: Tekhnika, 1975. 312 p.
15. P. Bond, S. Veerapaneni, Zeroing in on ZLD technologies for inland desalination, J. Am. Water Works Assoc., 100 (9) (2008), pp. 76-89
16. R. Bond, S. Veerapaneni, Zero Liquid Discharge for Inland Desalination, AWWA Research Foundation, Denver (2007), 233 pp.
17. Sung Ho Chae Joon Ha Kim, Chapter Four - Integration of PRO into Desalination Processes, Pressure Retarded Osmosis, Renewable Energy Generation and Recovery, 2017, Pages 129-151

Latin Symbols

| | |
|-------|---------------------------------------|
| A | Area, m |
| I | Energy gain, W/m^2 |
| c_p | Specific heat, J/kgK |
| x | Water salinity |
| g | Gravitational constant, m^2/s |
| r | Enthalpy of vaporization, kJ/kg |
| Q | Thermal power, W |
| Re | Reynolds number, <i>dimensionless</i> |
| I | Solar radiation rate, W/m^2 |

| | |
|-----|---|
| d | Diameter, m |
| P | Total system pressure, N/m^2 |
| G | Mass flow, kg/s |
| K | Overall heat transfer coefficient, W/m^2K |
| m | Mass flow rate, kg/s |
| s | Salt concentration, kg_{salt}/kg_{water} |
| P | Pressure, N/m^2 |
| W | Mass flow of evaporated water, kg/s |
| t | Temperature, K or $^{\circ}C$ |
| q | Heat flux density |

Greek Symbols

| | |
|----------------|---|
| α | Heat transfer coefficient, $W/m K$ |
| ν | kinetic viscosity, m^2/s |
| ε' | Emittance factor |
| Γ | Linear mass density of irrigation, $kg/s m$ |
| Π | Wetted perimeter, m |
| μ | Dynamic viscosity, $kg/m.s$ |
| ρ | Density, kg/m^3 |
| λ | Thermal conductivity, W/mK |
| Δt | Temperature difference, $^{\circ}C$ |
| δ | Thickness, m |

Subscripts

| | |
|--------|--------------------------|
| w | water |
| sw | sea water |
| $conc$ | concentrate |
| $wall$ | wall |
| wc | water solar collector |
| sec | secondary |
| $wast$ | wastage |
| d | hydration |
| out | out |
| ev | evaporation |
| sat | temperature of saturated |
| dep | deposition |

Acronyms and abbreviations

| | |
|----------|--|
| ZLD | zero liquid discharge |
| DFE | drum film evaporator |
| DFEM | drum film evaporator module |
| sSDP-DFE | Self-Powered Solar Desalination Plant based on Drum Film Evaporators |
| SWRO | Sea Water Reverse Osmosis |
| MSE | Multi-stage evaporation |
| SEC | specific energy consumption |
| MSF | Multi-Stage Flash |
| RO | reverse osmosis |
| MED | Multiple-effect distillation or multi-effect distillation |

TVC
SV

Thermal vapor compression
Solenoid valve